[SSC21-XIII-04]

Ballistic Aerocapture for SmallSat: A Case Study for Venus Atmospheric Sampling Probe

Oswaldo Santana, Ye Lu
Kent State University
1400 Lefton Esplanade, Kent, OH
osantana@kent.edu, ylu16@kent.edu

ABSTRACT

Aerocapture is a maneuver that can improve the capabilities of interplanetary small satellite missions to efficiently deliver a probe to a target destination. The maneuver is accomplished with a single atmospheric pass followed by a small propulsive burn to reach the final orbit. In this paper, we consider a SmallSat atmospheric sampling probe with an existing heatshield and evaluate the performance and benefits of ballistic aerocapture. The performance is assessed by comparing ΔV required of a fully propulsive orbital insertion and that of a ballistic aerocapture. Significant fuel mass savings can be achieved with a passive lifting vehicle. With a sample case of arrival V_∞ of 4 km/s, vehicle ballistic coefficient of 200 kg/m^2, and lift-to-drag ratio (L/D) from 0 to 0.5, the results show a 99-percentile ΔV saving of 30 m/s for L/D of 0, 1700 m/s for 0.2, and 2600 m/s for 0.4 and peak heat rate of about 100–750 W/cm^2, a peak total heat load of about 4–20 kJ/cm^2, and a peak deceleration load of up to 18 Earth's G.

INTRODUCTION

Aerocapture is a promising orbital insertion maneuver that can be used in missions to any atmosphere-bearing body. Previous studies have shown that aerocapture can provide either a short time-of-flight, a higher delivered payload, or both.[1] Aerocapture allows for a mass saving from the reduction of the typical propulsive engine-fuel system. However, performing an aerocapture maneuver requires specific design considerations that are similar to an entry vehicle.

The conventional benefit trade-off between aerocapture and other orbit insertion maneuvers is between the added mass of the thermal protection system (TPS) and the propellant mass required for fully propulsive orbit insertion. However, such comparison is inadequate in the case where the probe has already equipped a heatshield (for example, an atmospheric sampling probe). The probe may be able to perform an aerocapture maneuver without major design changes. Ultimately, aerocapture could help reduce the total mass required to perform the initial orbital insertion and may enable a certain class of small satellite missions.

Ballistic aerocapture requires the probe to arrive at a "safe" entry flight-path angle as shown in Figure 1. With perfect knowledge of all conditions (i.e., atmospheric density, vehicle aerodynamics, etc.), the maneuver is still very sensitive to the entry conditions—the probe may "crash" if the entry flight-path angle is too steep.[2] Achieving a captured orbit can be challenging without trajectory control, and the probe may also escape after the atmospheric pass. Thus, a post-aerocapture trajectory correction maneuver (TCM) is needed to reach the target orbit. The main advantage of ballistic aerocapture is the simplicity in probe design and operation (i.e., a passive lifting rigid body), whereas aerocapture in the literature requires some trajectory controls onboard, such as additional thrusters for banking maneuver.[3]

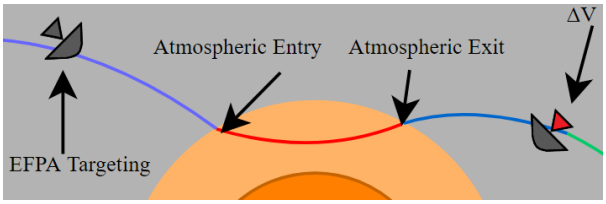

Figure 1: Schematic of Ballistic Aerocapture

Performance of ballistic aerocapture depends on probe aerodynamics, arrival conditions, and atmospheric densities. For probes with a heatshield that is designed for the prime mission (for example, to withstand heating during atmospheric samples collection), the heatshield may have a limiting heat rate that is insufficient for aerocapture. Thus, we need to ensure the probe can survive the ballistic aerocapture in terms of the peak heat rate. If ablative TPS material is used, the total heat load must also be considered when designing the thickness of the heatshield. Ballistic aerocapture may add some mass to the existing heatshield if design changes are needed, meanwhile reducing the propellant mass required. For the heatshield, allowable peak heat rate and total heat load are the key considerations. The aerothermal heating conditions depend on the atmospheric entry velocity (or

the approach velocity), probe lift-to-drag ratio, ballistic coefficients, and atmospheric density profile.[4]

Applicable Mission Concept

One mission concept that may be suited for ballistic aerocapture is Cupid's Arrow—a small spacecraft mission concept shown in Figure 2.[5] The proposed mission is to determine the noble gas composition of Venus' atmosphere. The Cupid's Arrow probe is designed with a heatshield that would protect it from atmospheric heating while collecting atmospheric samples.

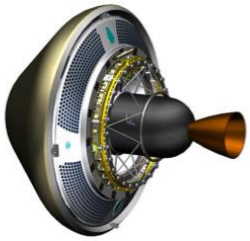

Figure 2: Concept Cupid's Arrow Vehicle[5]

The Cupid's Arrow mission concept is an example where ballistic aerocapture may be used. Ballistic aerocapture may also benefit traditional missions with high arrival velocities by potentially increasing the payload mass or reducing the total mass for launch.

MATHEMATICAL MODELS

Planar Equations of Motion

Ballistic aerocapture follows atmospheric flight dynamics when the vehicle is below the atmospheric interface[6], assumed to be 180 km altitude. We consider planar equations of motion without planet rotation and gravity perturbations since J2 and J4 are small for Venus which are negligible for aerocapture maneuver. In addition, wind speed is not included due to its dependence on interplanetary transfer trajectory. The equations of motion are as follows:

$$\dot{V} = -\frac{q}{\beta} + g_r \sin\gamma \tag{1a}$$

$$\dot{\gamma} = \frac{q(L/D)}{V\beta}\cos\sigma + \frac{g_r \cos\gamma}{V} \tag{1b}$$

$$\dot{\theta} = \frac{V\cos\gamma}{r} \tag{1c}$$

$$\dot{r} = V\sin\gamma \tag{1d}$$

where V is the planet-relative velocity, γ is the flight path angle, θ is the longitude equivalent, and r is the radius. σ is the bank angle, $q = 1/2\rho V^2$ is the dynamic pressure, ρ is the atmospheric density which is modeled after Venus International Reference Atmosphere (VIRA), $\beta = m/C_d A$ is the ballistic coefficient, where C_d is the drag coefficient, and A is the reference drag area. $g_r = \mu/r^2$ is the radial gravitation acceleration, L/D is the lift-to-drag ratio.

Keplerian Orbits

For the flight that is above the atmospheric interface, we assume a simplified two-body model where the vehicle follows Keplerian orbital motion with the following analytical equations:

$$\varepsilon = \frac{V^2}{2} - \frac{\mu}{r} = -\frac{\mu}{2a} \tag{2}$$

$$h = rV\cos(\gamma) \tag{3}$$

$$e = \sqrt{1 - h^2/(\mu a)}, \text{ elliptical orbit} \tag{4}$$

$$r_a = a(1+e), \text{ elliptical orbit} \tag{5}$$

where h is the specific angular momentum, e is the eccentricity of the orbit, a is the semimajor axis of the orbit, and r_a is apoapsis radius.

Aerothermodynamic Heating

Radiative and convective heat rates during aerocapture are obtained from empirical relations. The convective heat rate follows the Sutton-Grave formulation[7]:

$$\dot{q}_c = k(\rho_\infty/R_n)^{0.5}V^3 \tag{6}$$

where k=1.896×10^{-8} is an empirically determined constant, R_n is the nose radius, assumed to be 1 m as the baseline. Radiative heat rates are also found as follows:

$$\dot{q}_r = k_1\rho_\infty^{1.2}V^{10.0}R_n^{0.49} \qquad V > 8 \text{ km/s} \tag{7a}$$

$$\dot{q}_r = k_2\rho_\infty^{1.2}V^{5.5}R_n^{0.49} \qquad 8 \text{ km/s} < V < 10 \text{ km/s} \tag{7b}$$

$$\dot{q}_r = k_3\rho_\infty^{1.2}V^{13.4}R_n^{0.49} \qquad 10 \text{ km/s} < V < 12 \text{ km/s} \tag{7c}$$

where k_1=3.33×10^{-34}, k_2=1.22×10^{-16} and k_3= 3.07×10^{-48}. The total heat rate $\dot{q}_{\text{total}}$ is the sum of convective and radiative heat rates as follows:

$$\dot{q}_{\text{total}} = \dot{q}_c + \dot{q}_r \tag{8}$$

The total heat load Q is the integral of total heat rate over the duration of the atmospheric pass:

$$Q = \int_0^t \dot{q}_{\text{total}}\, dt \tag{9}$$

METHODOLOGY

To assess the performance of ballistic aerocapture, we use a two-step process to determine the proper arrival conditions to ensure a successful maneuver. The first step is finding the nominal entry condition based on the average unperturbed atmospheric density, nominal arrival velocity, and nominal vehicle aerodynamics. The second step is to find the practical entry conditions using Monte Carlo simulation considering expected perturbations such as atmospheric density variation, vehicle aerodynamics, and interplanetary navigation.

Nominal Entry Condition

Nominal entry condition for a successful aerocapture maneuver is determined through iterations over entry flight-path angle (EFPA) using the bisection method. To find the nominal EFPA, denoted by γ_0, the motion of the vehicle is modelled and simulated numerically using equation 1. Equations 2–5 are used to characterize the post aerocapture orbit, i.e., r_a. γ_0 is iterated until the target apoapsis radius is met from the exit conditions.

Perturbations and Monte Carlo Simulation

Major perturbations are considered and modeled in the simulation. The entry velocity, entry altitude, ballistic coefficient, L/D, and atmospheric density all have uncertainties thus they are varied assuming a Gaussian distribution which are all listed in Table 1.

Table 1: Nominal Parameters and Uncertainties

Parameter	Nominal	Variation	3σ
Entry Velocity	10.9 km/s	Gaussian	3%
Entry Altitude	180 km	Gaussian	3 km
Ballistic Coefficient	200 kg/m^2	Gaussian	15%
L/D	0 – 0.4	Gaussian	10%
Density	VIRA	Gaussian	0–60% *

Nominal entry velocity of 10.9 km/s corresponds to a V_∞ of 4 km/s. Each parameter is perturbed about the nominal values with a Gaussian distribution and remains constant in each simulation. The 3σ variation of atmospheric density varies linearly with the altitude (from 60% at 180 km to 0% at surface) as shown in Figure 3. The vertical line at 1 denotes the nominal atmospheric density, upper and lower bounds are shown in red, and 50 random atmospheric profiles are also generated as illustration.

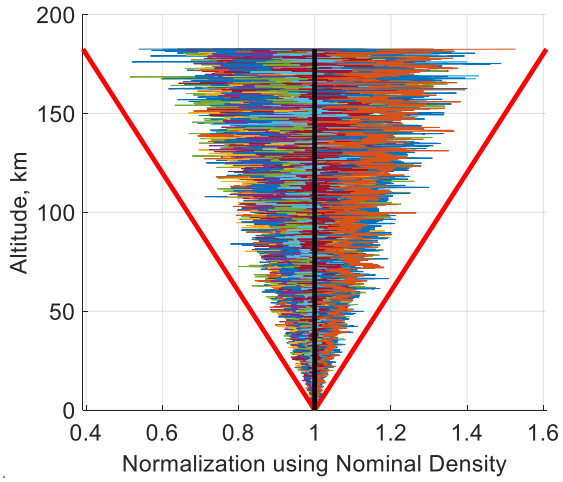

Figure 3: Atmospheric Density Modeling and Perturbation

Monte Carlo simulation uses the perturbed parameters as noted in Table 1 and repeats the simulation 1000 times for each set of nominal values.

Adjusted Entry Conditions

Since the nominal γ_0 does not account for the perturbations, any variations during the actual flight may cause the vehicle to deviate from the desired path, which may eventually cause a crash. In order to achieve 100% success (non-crash), we need to determine a practical entry condition via Monte Carlo analysis, which uses the nominal γ_0 as an initial guess and simulates the maneuver using a range of flight-path angles to determine the critical value needed for 100% success. The critical value is the adjusted EFPA, denoted by γ_e, which will guarantee a 100% success under realistic conditions.

Optimal Two-Impulse ΔV

Ballistic aerocapture can provide mass saving but does not eliminate the need for propulsive ΔV. After the atmospheric pass, a minimum of two impulses are needed for post-aerocapture orbit correction. The first ΔV immediately or shortly after exiting atmospheric interface adjusts the apoapsis radius. The second ΔV is executed at apoapsis to raise the periapsis out of the atmosphere and to the final target orbit. Assuming Keplerian orbit, equations used to calculate the ΔV are as follows:

* 3σ varies linearly at surface from 0% of nominal density to 60% at entry altitude.

$$\Delta V_1 = \sqrt{{V_{ex}}^2 + {V_t}^2 - 2V_{ex}V_t \cos(\gamma_{ex} - \gamma_t)} \quad (10)$$

$$\Delta V_2 = \sqrt{\frac{2\mu}{R_a} - \frac{2\mu}{r_{p,t} + r_{a,t}}} - V_{a,t} \quad (11)$$

$$\Delta V_{AC} = \Delta V_1 + \Delta V_2 \quad (12)$$

where V_{ex} is the exit velocity, V_t is the velocity of the transfer orbit, γ_{ex} is the exit flight-path angle, γ_t is the flight path angle for the transfer orbit, R_a is the apoapsis of the target orbit, $r_{a,t}$ and $r_{p,t}$ are the apoapsis and periapsis radius of the target orbit, and $V_{a,t}$ is the velocity at apoapsis of the transfer orbit.

V_t and γ_t depend on the characteristics of the transfer orbit, which can be expressed using a single variable, periapsis radius of the transfer orbit $r_{p,t}$ as follows:

$$V_t = \sqrt{\frac{-2\mu}{r_{p,t} + r_{a,t}} + \frac{2\mu}{r_{ex}}} \quad (13)$$

$$\gamma_t = \cos^{-1} \frac{\sqrt{2\mu}\sqrt{\frac{r_{p,t}\, r_{a,t}}{r_{p,t} + r_{a,t}}}}{r_{ex}V_t} \quad (14)$$

The transfer orbit has the same apoapsis radius as the target orbit, therefore $r_{a,t} = R_a$ which is known and r_{ex} is the radius of atmospheric interface. ΔV_{AC} is then only a function of $r_{p,t}$, which is minimized by letting:

$$\frac{d\Delta V_{AC}}{dr_{p,t}} = 0 \quad (15)$$

To evaluate the effectiveness of ballistic aerocapture, we compare the optimal two-impulse ΔV_{AC} with the ΔV needed from fully propulsive orbit insertion.

The fully propulsive insertion is minimized by assuming the ΔV is performed at target periapsis radius. A single ΔV will transfer the vehicle to the target orbit:

$$\Delta V_{\text{prop}} = \sqrt{\frac{2\mu}{R_p} - V_\infty^2} - \sqrt{\frac{2\mu}{R_p} - \frac{2\mu}{r_{p,t} + r_{a,t}}} \quad (16)$$

where R_p is the periapsis radius of the target orbit.

NUMERICAL RESULTS

Nominal EFPA

The nominal γ_0 depends on both V_∞, vehicle ballistic coefficient, and L/D, and is also related to the target apoapsis radius. For non-zero L/D, the direction of the lift vector has a significant impact on the sensitivity to EFPA. Figure 4 shows the nominal γ_0 for both lift-up and lift-down configurations with vehicle L/D of 0.2 and 0.4. The range of EFPA is very minimal for lift-down configuration, meaning that very small change in any variable will cause the vehicle crash or escape. However, for lift-up, there is a reasonable range of EFPA that may be sufficient to accommodate uncertainties. In the following, we will assume the vehicle flies a passive lift-up configuration for non-zero L/D.

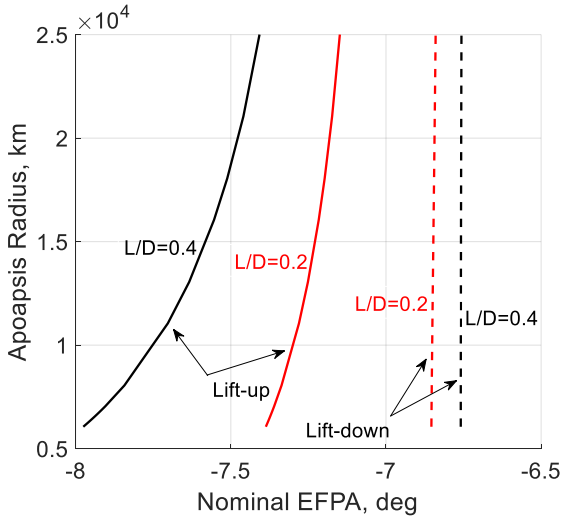

Figure 4: Nominal EFPA for Lift-up and Lift-down Configurations with Entry Velocity of 10.9 km/s.

Figure 5 shows the relation between the nominal γ_0 and the target apoapsis at different ballistic coefficients with L/D of 0. Figure 5 also shows the theoretical maximum and minimum EFPA for β = 200 kg/m^2, that correspond to the critical values for non-crashing and non-escaping, that is, a steeper EFPA will cause the vehicle not exiting the atmosphere, hence a crash; whereas a shallower EFPA produces very minimum deceleration, resulting in an escape.

Figure 6 shows the same detail as Figure 5 but for L/D of 0.2. Due to an increase in lifting capability, the ranges of EFPA for L/D of 0.2 are general steeper than that of L/D of 0. As L/D increases, the nominal γ_0 will become steeper.

To define the nominal γ_0, we will use a target apoapsis of 56,000 km (equivalent altitude of 50,000 km) for all following results.

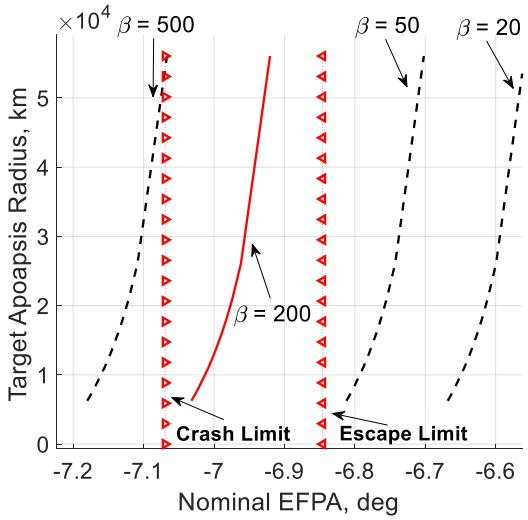

Figure 5: Target Apoapsis vs Nominal EFPA for L/D of 0

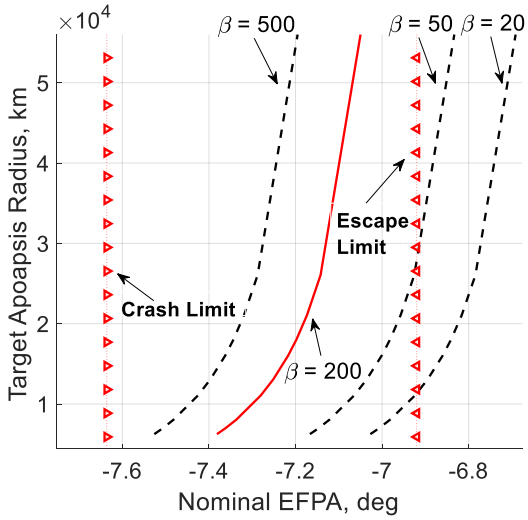

Figure 6: Target Apoapsis vs Nominal EFPA for L/D of 0.2

Adjusted EFPA

The adjusted γ_e represents the practical value that depends on the uncertainties of environmental and vehicle parameters. Using Monte Carlo simulation, Figure 7 shows the comparison between the nominal and adjusted EFPA for vehicle L/D from 0 to 0.5.

The nominal γ_0 for each L/D allows the vehicle to exit the atmosphere and arrive at the target apoapsis radius. As shown in Figure 7, for L/D of 0, the adjusted γ_e is shallower than γ_0 and as L/D increases, the adjusted γ_e can be steeper than the nominal γ_0. It is important to note that adjusted γ_e does not target for a specific orbit and can be considered as the critical EFPA that is required for 100% non-crash. Any EFPA that is shallower than γ_e will also result in 100% non-crash. However, due to the need for high deceleration, a steeper angle is usually preferred. Table 2 lists the nominal and adjusted EFPA which are used in the following results.

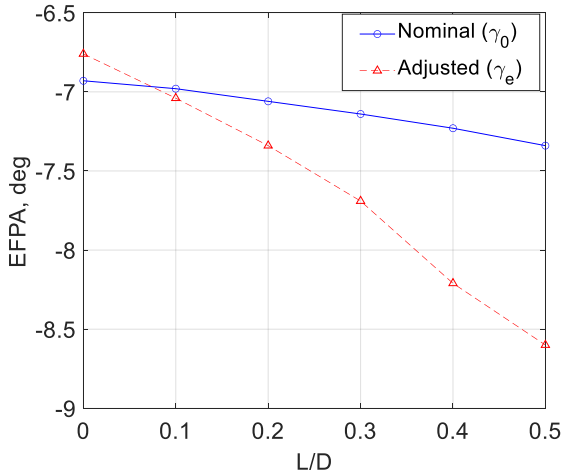

Figure 7: Nominal and Adjusted EFPA for L/D from 0 to 0.5

Table 2: Selected Nominal and Adjusted EFPA

L/D	Nominal γ_0	Adjusted γ_e
0	−6.9°	−6.7°
0.2	−7.0°	−7.3°
0.4	−7.2°	−8.2°

ΔV Saving

Using the adjusted γ_e, we assess the performance of ballistic aerocapture by comparing the ΔV of aerocapture with that of fully propulsive orbit insertion. Using Monte Carlo analysis, we perturbed the uncertain parameters and numerically simulated the atmospheric trajectory 1000 times for each L/D.

Figure 8 shows the distributions of ΔV saving of ballistic aerocapture for L/D of 0, 0.2 and 0.4 respectively. Positive ΔV saving means that ballistic aerocapture is more efficient. We notice a significant improvement of ΔV savings by incorporating some passive lifting capability. As L/D increases, the ΔV savings are more concentrated about the average.

Table 3 lists the mean, minimum, maximum, and standard deviations for the results shown in Figure 8 as well as the actual ΔV from aerocapture and fully propulsive orbit insertion.

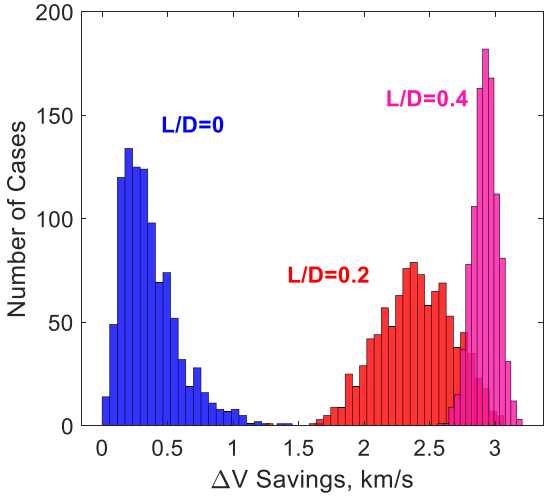

Figure 8: Histograms of ΔV Savings

Table 3: Statistics of ΔV in m/s

Parameter	L/D		
	0	0.2	0.4
ΔV saving, mean	367	2398	2924
ΔV saving, min.	32	1707	2671
ΔV saving, max.	1195	3011	3149
ΔV saving, std.	209	277	91

Although, for L/D of 0, the mean ΔV saving is more than 300 m/s, when designing the vehicle, we need to consider the 99-percentile ΔV saving, i.e., equivalently the minimum values in Table 3. As L/D increases, ΔV saving is more significant at over 1700 m/s 99-percentile for L/D of 0.2, and over 2600 m/s for 0.4.

Structural and Thermal Loads

We also evaluated the peak heat rate, total heat load, and peak deceleration to demonstrate the structural and thermal loads on the vehicle. The results shown in this section are consistent with ΔV saving.

Figures 9–11 show ΔV saving vs peak heat rates, total heat load, and peak g-load respectively for all 1000 runs of Monte Carlo simulation with L/D of 0, 0.2, and 0.4. The blue points correspond to a L/D of 0, red plus markers for L/D of 0.2, and magenta star markers for a L/D of 0.4. It is important to note that the adjusted γ_e with 100% non-crashing rate is used. Also, for some cases with L/D of 0, ballistic aerocapture only provides a very small deceleration and the vehicle will exit the atmosphere on an escape orbit, resulting in very minimal ΔV saving.

As expected, there is a positive correlation between the ΔV savings and peak heat rate, total heat load, and peak g-load. More ΔV saving means higher peak heat rate, higher total heat load, and higher peak deceleration.

From Figure 9, we notice that as L/D increases, the peak heat rate increases significantly, yet is reasonable compared with the state-of-the-art TPS materials. Heat rates experienced during the atmospheric pass for high ΔV savings increase with increased vehicle L/D which is also a result of high deceleration as shown in Figure 11. The total heat load in Figure 10 shows an interesting result where for L/D of 0.4, the total heat load is roughly the same as that for L/D of 0.2. From the design perspective, total heat load is positively correlated with the total mass fraction for the heatshield. Assuming that the same TPS materials are used for both L/D of 0.2 and 0.4, an increase in L/D will result in a higher ΔV saving meanwhile requiring no increase in heatshield mass.

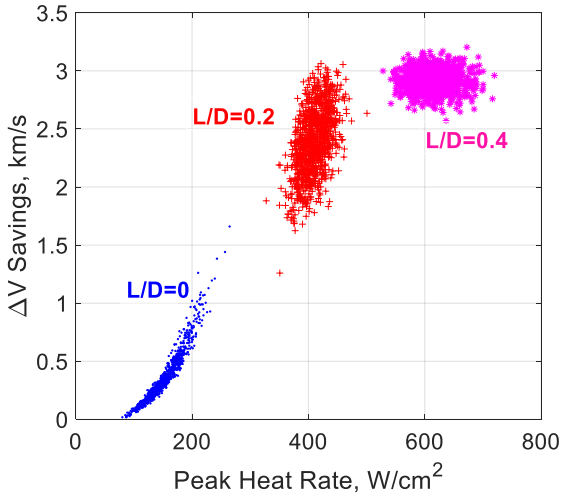

Figure 9: Heat Rate and ΔV Savings

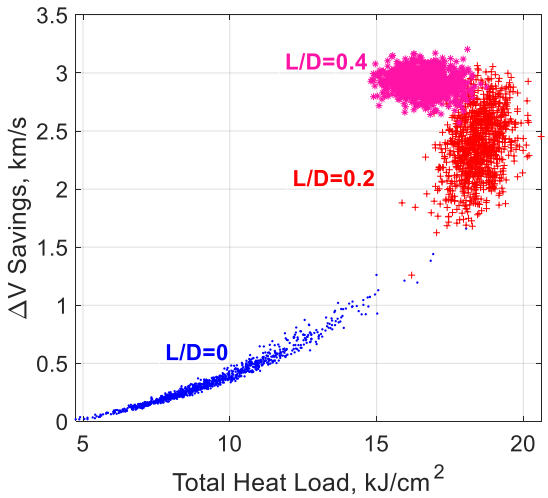

Figure 10: Total Heat Load and ΔV Savings

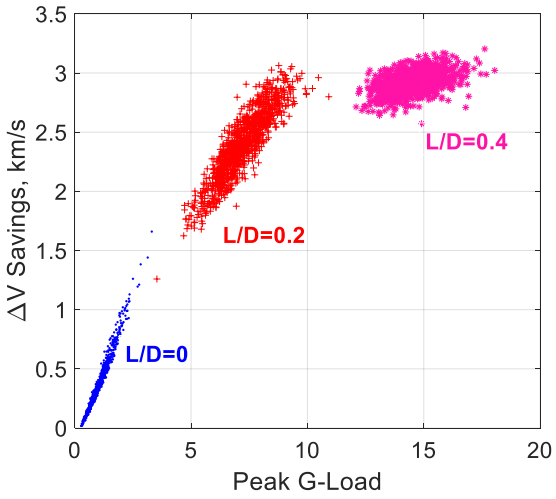

Figure 11: Peak G-Load and ΔV Savings

SUMMARY

Ballistic aerocapture maneuver can be used to reduce the total ΔV necessary to deliver a probe into orbit. Using the assumed arrival condition, we have shown that the deceleration and thermal loads are reasonable. The peak heat rate of the aerocapture maneuver is within the capability of currently available TPS materials. A slightly increase in the vehicle aerodynamic L/D can also allow for a significant improvement in performance.

Using Monte Carlo simulations, adjusted γ_e is found which considers perturbations in entry velocity, entry altitude, ballistic coefficient, L/D, and atmospheric density. A minimal control strategy allows for the maneuver to increase mass margins through ΔV savings while ensuring the probe survives the atmospheric pass by properly targeting the entry flight path angle.

A probe with a passive lift-up design will be able to attain more ΔV savings than a non-lifting vehicle, but both are able to safely perform the maneuver with very minimal risk. Ballistic aerocapture can provide potentially significant mass savings when probe and mission design are thoroughly evaluated.

REFERENCES

1. Saikia, S. J., Millane, J., Lu, Y., Mudek, A., Arora, A., Witsberger, P., Hughes, K., Longuski, J. M., Spilker, T., Petropoulos, A., Arora, N., Cutts, J., Elliott, J., Sims, J., and Reh, K., "Aerocapture Assessment for NASA Ice Giants Pre-Decadal Survey Mission Study," Journal of Spacecraft and Rockets, vol. 58, Mar. 2021, pp. 505–515.
2. Vinh, N. X., Johannesen, J. R., Longuski, J. M., and Hanson, J. M., "Second-Order Analytic Solutions for Aerocapture and Ballistic Fly-Through Trajectories," The Journal of the Astronautical Sciences, Vol. 32, 1984, pp. 429–445.
3. Lu, Y., and Saikia, S. J., "Feasibility Assessment of Aerocapture for Future Titan Orbiter Missions," Journal of Spacecraft and Rockets, vol. 55, 2018, pp. 1125–1135.
4. Girija, A. P., Lu, Y., and Saikia, S. J., "Feasibility and Mass-Benefit Analysis of Aerocapture for Missions to Venus," Journal of Spacecraft and Rockets, Vol. 57, No. 1, 2020, pp. 58–73
5. Sotin, C., Avice, G., Baker, J., Freeman, A., Madzunkov, S., Stevenson, T., Arora, N., Darrach, M., Lightsey, G., and Marty, B., "Cupid's arrow: a small satellite concept to measure noble gases in Venus' atmosphere,"49th Lunar and Planetary Science Conference, 2018.
6. Miele, A., Zhao, Z. G., and Lee, W. Y., "Optimal Trajectories for the Aeroassisted Flight Experiment. Part 1: Equations of Motion in an Earth-fixed System," Tech. rep., Rice University, 1989.
7. Page, W. A., and Woodward, H. T., "Radiative and convective heating during Venus entry." AIAA Journal, Vol. 10, No. 10, 1972, pp. 1379–1381.